Chapter 2
Phase Behavior of Biomass Components in Supercritical Water

Sergey Artemenko, Victor Mazur, and Pieter Krijgsman

Success depends upon previous preparation, and without such preparation there is sure to be failure.

Confucius

Abstract The importance of thermodynamic and phase behavior is fundamental to supercritical water (SCW) technologies of biomass treatment. Considering the extremely large number of biomass components, it is obvious that there is need for developing theoretically sound methods of the prompt estimation of their phase behavior in aquatic media at supercritical conditions. A local mapping concept is introduced to describe thermodynamically consistently the saturation curve of water and biomass components. The global phase diagram studies of binary mixtures provide some basic ideas of how the required methods can be developed to visualize the phase behavior of biomass decomposition products in supercritical aqueous media. The mapping of the global equilibrium surface in the parameter space of the equation of state (EoS) model provides the most comprehensive system of criteria for predicting binary mixture phase behavior. Analytical expressions for selection the azeotropic states in binary mixtures are given. Results of calculations of phase equilibria and critical curves for main biomass components in supercritical water are described.

S. Artemenko • V. Mazur (✉)
Institute of Refrigeration, Cryotechnologies, and Eco-Power Engineering (former Academy of Refrigeration), Odessa National Academy of Food Technologies, 1/3 Dvoryanskaya Str., 65082 Odessa, Ukraine
e-mail: mazur@paco.net

P. Krijgsman
Ceramic Oxides International, Wapenveld, The Netherlands
e-mail: p.krijgsman@cerox.nl

Z. Fang and C. Xu (eds.), *Near-critical and Supercritical Water and Their Applications for Biorefineries*, Biofuels and Biorefineries 2, DOI 10.1007/978-94-017-8923-3_2,

Keywords Biomass components • Supercritical water • Widom line • Phase equilibria • Global phase diagram • Parameter identification

2.1 Introduction

Biomass is the prevailing form of renewable energy which can provide the conversion to heat and power, biofuels and biobased chemicals as the replacement of conventional fossil. Three key macromolecules: lignin, cellulose, and triacylglycerides can generate the wide opportunities to transform biomass into goal products – energy and desired materials [1]. Proteins are not primary components of biomass and account for a lower proportion than do the previous three macromolecules.

Protein properties depend on the kinds and ratios of constituent amino acids, and the degree of polymerization. The amounts of the other organic components vary widely depending on specie, but there are also organic components. Biomass comprises organic macromolecular compounds, but it also contains inorganic substances (ash) in trace amounts. The primary metal elements include Ca, K, P, Mg, Si, Al, Fe, and Na.

There are many classical technologies that ensure the fulfillment of biomass conversion problem but modern challenges of sustainable development require the emergence of environmentally friendly green technologies. Water in supercritical state i.e. at temperature and pressure high enough to vanish differences between liquid and vapor phases, above 647 K and 22 MPa, is recognized as green solvent. Thermodynamic and phase behavior of SCW are differed qualitatively from the "normal" state (for example it can act as a quasi-organic solvent). Not only the chemistry, but also the physics can change drastically. For example, density variation with a factor of 7 for 25 MPa around a few Kelvin range in the supercritical region across the Widom line representing the maximum of response functions can change heat capacity and compressibility with several order of magnitudes, making almost impossible to use traditional flow- and thermal transport calculations. Development of new SCW technologies is impeded by the lack of fundamental understanding of many aspects of the supercritical fluid state itself, and particularly of their thermodynamic and phase behavior. Properties and phase equilibria of fluid mixtures define the scientific platform for developing green chemical processes and predetermine the success of emergent technologies [2].

The main aim of this Chapter is to review existing experimental data and theoretical models for analyzing, correlating, and predicting the phase behavior of biomass components in supercritical water.

The Chapter is organized as follows. In the first section, main biomass components are selected. Critical (or pseudocritical) parameters are considered as fundamental characteristics of a fluid by themselves and also often as the input from which the other physical properties can be generated. The quantitative structure-property relationships (QSPRs) to estimate the critical properties of biomass components are discussed. The boundaries of the Widom line for supercritical water

where reaction mechanisms accelerate the biomass conversion maximally are given. In the second part, a theoretical analysis of the topology of phase diagrams as useful tool for understanding the phenomena of phase equilibrium that are observed in biomass components – supercritical water mixtures in vicinity of the Widom line is given. We review the global phase behavior of binary mixtures and derive an analytical expression for determining the boundaries of azeotropy in terms of the critical parameters of mixture components and the binary interaction parameter k_{12} for the one fluid models of the equation of state. The knowledge of binary interaction gives possibility to predict all types of phase behavior in supercritical water – biomass component mixtures. The results of simulation of phase equilibria for binary mixtures are illustrated using examples of various classes of biomass components.

2.2 Main Biomass Components

The estimation of the properties of main biomass components is an important prerequisite for the design of processes and equipment, environmental impact assessment and other major chemical engineering activities related to phase equilibria. The main components of biomass resources are typically 40–45 wt% cellulose, 25–35 wt%, hemicellulose, 15–30 wt% lignin and up to 10 wt% for other compounds [3]. Elemental composition of conventional biomass includes following components: C, H, O, N, and S. Chemical formula $C_aH_bO_cN_dS_e$ simulates the various types of biomass, e.g., sewage sludge $C_{2.83}H_{4.86}O_{1.25}N_{0.34}S_{0.04}$, microalga Spirulina $C_{3.66}H_{6.81}O_{2.16}N_{0.47}S_{0.01}$, the zoomass $CH_{2.06}$ $O_{0.52}N_{0.12}S_{0.01}$, and others [4]. Possible reaction products depend on goals of biomass conversion and thermodynamic conditions of SCW treatment processes. The gasification of biomass and organic wastes generates the gas components such as H_2O, CO_2, CO, N_2, N_2O, NO, NO_2, SO_2, SO_3, H_2, CH_4, and hydrocarbons (HC). Biomass products produced from different materials and by different external conditions may differ greatly from one another. As a result, the compositions of different reaction products usually vary in wide ranges.

To establish the thermodynamic properties of great variety of compounds under SCW treatment the simple models of the EoS $P = P\,(T,V,X)$, e.g., the Peng-Robinson (PR) [5] or the Redlich-Kwong-Soave (SRK) [6, 7] models are a better choice to link key characteristics of biomass components and target properties. Critical parameters of biomass components can be considered as their information characteristics which could generate a set of target properties for designed SCW system. This class of EoS has simple relationships between their model parameters and critical constants derived from critical conditions. During the many years of super critical research, a variety of fluids have been investigated, and accordingly, both their critical temperature and pressure have been determined. An exposure of these physical properties is condensed in Table 2.1.

Table 2.1 Critical properties of selected chemical compounds (sorted by critical temperatures)

Product components	Critical temperature, (K)	Critical pressure (MPa)	Critical density (kg/m^3)	Acentric factor
Hydrogen	33.145	1.296	31.26	−0.219
Nitrogen	126.19	3.396	313	0.0372
Carbon monoxide	132.86	3.444	303.91	0.0497
Oxygen	154.60	5.013	436.14	0.0222
Methane	190.56	4.599	162.66	0.0114
Ethylene	282.16	5.042	214.25	0.0866
Carbon dioxide	304.13	7.377	467.6	0.2239
Ethane	305.46	4.872	206.18	0.0995
Propane	309.52	4.251	228.48	0.1521
Nitrous oxide	369.90	7.245	452	0.1613
Ammonia	405.40	11.333	225	0.2560
Sulfur dioxide	430.64	7.884	525	0.2557
Sulfuric oxide	491.00	8.200	630	0.4810
Ethanol	513.90	6.148	276	0.6440
Water	647.096	22.064	322	0.3443

To define more exactly equation of state parameters for pure substances, especially for water, concept of local mapping is developed. Standard approach to determination of the EoS parameters $\boldsymbol{X} = X\ (a,\ b,\ \alpha)$ is derived from critical conditions. But for phase equilibria prediction this parameter set is not sufficient to satisfy the limiting conditions for pure components ($x \to 1$ and $x \to 0$). To provide a reliable thermodynamic consistency between exact and model equations of state the equalities of pressures, isothermal compressibility's and internal energies should be applied. As an example, a refinement of the SRK EoS parameters is considered. To satisfy thermodynamic consistency conditions at given point of $P - V - T$ surface the set of equations (2.1) should be solved:

$$\begin{aligned} P_{exact}(T,V) - P_{mod}(X,T,V) &= 0, \\ \frac{\partial P_{exact}(T,V)}{\partial T} - \frac{\partial P_{mod}(X,T,V)}{\partial T} &= 0, \\ \frac{\partial P_{exact}(T,V)}{\partial V} - \frac{\partial P_{mod}(X,T,V)}{\partial V} &= 0 \end{aligned} \tag{2.1}$$

where P_{exact} – fundamental EoS for H_2O [8], P_{mod} – the SRK model [7], $\boldsymbol{X}$ – vector of the SRK model parameters, $\alpha(T/Tc,\omega)$ as function of reduced temperature and acentric factor (ω) is the attractive term in the original Redlich–Kwong equation. Results of calculations, which exactly describe data along saturation curve, are presented in Table 2.2.

More sound consideration of problem should be guided on quantitative "structure – property" relationships (QSPR). The basic idea of QSPR is to find a

Table 2.2 Parameters of the SRK EoS for water

T, K	P, MPa	V_l, cm^3/mole	a_{H_2O}, J·m^3/mole^2	b_{H_2O}, cm^3/mole	α
400	0.24577	19.217	0.49846	14.542	0.92771
450	0.93220	20.234	0.44438	14.612	1.0563
500	2.6392	21.671	0.42379	14.628	1.0922
550	6.1172	23.836	0.40995	14.515	1.0812
600	12.345	27.741	0.39366	14.141	1.0466

relationship between the structure of compound expressed in terms of constitutional, geometrical, topological, and other quantum-chemistry descriptors and target property of interest.

The QSPR employs two databases – the critical property database and structure database. The correlations between databases are established in the form of the property model – ***M(P)***, the parameters of which are determined by minimizing the "distance" between the experimental property $\boldsymbol{P}_j$ and its model ***Mj***. For the most of compounds experimental data are available via on-line databanks e.g., NIST, KDB, CHEMSAFE, BEILSTEIN, GMELIN et al. If direct measurement results are not in option, thermodynamic models from process simulators like ASPEN PLUS can be partly used to estimate the missing properties.

There are many group contribution methods estimating the critical properties of possible biomass compounds from molecular structure and success of any model depends on the amount of data used in determining the contribution of independent variables (molecular descriptors). The start point of group contribution technique is a decomposition of the molecular structure into particular groups and the counting of atoms in those groups. Increments are assigned to the groups by regression of known experimental data for the chosen property. The molecular structure can be retrieved by summation of the contributions of all groups. The least sophisticated atom count technique was proposed by Joback [9]. More general cases for molecular descriptors determination are described elsewhere, e.g. [10, 11]. At present time reliable correlations are established by heuristic, Multi-Linear Regression techniques, e.g. [12], by nonlinear techniques like Genetic Function Approximation [13] or by Artificial Neural Networks, e.g. [14]. The choice of appropriate technique to predict critical properties from molecular structure depends on the statement problem and should correspond to the final aim of molecular design. Distribution of critical points for hydrocarbons and key biomass components versus saturation curve of water are given in Fig. 2.1.

Critical temperature and pressure data for the hydrocarbons were taken from correlation Wakeham et al. [15]. Data for selected chemical compounds were taken from Table 2.1. Critical (or pseudocritical) parameters are considered as fundamental characteristics of a fluid by themselves and also often as the input from which the other physical properties can be generated. The chain starting from descriptors of molecular structure to target property of biomass components should be constructed through critical parameters of technological fluid and equation of state model, accordingly.

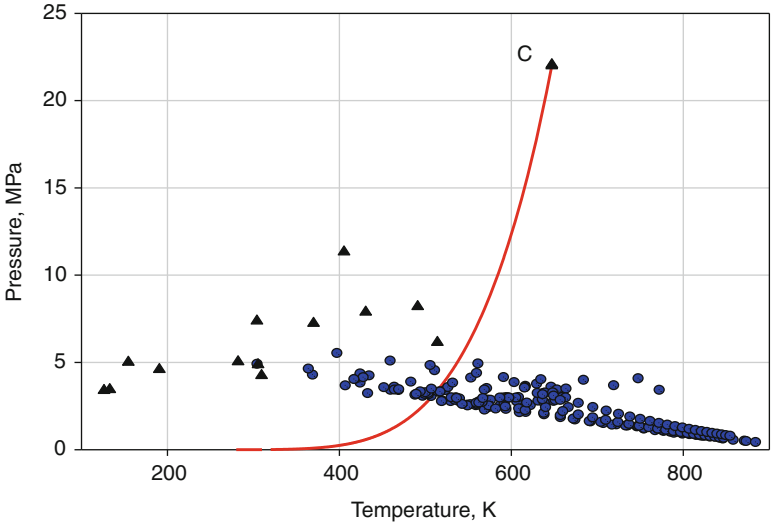

Fig. 2.1 Distribution of critical points of hydrocarbons (●) and selected chemical compounds (▲) versus location of H_2O saturation curve

2.3 SCW Thermodynamic Behavior

The critical point defines the vertex of the vaporization boundary; hence, geometric considerations ensure that isothermal compressibility, isobaric expansion and other specific partial derivatives will diverge to infinity at critical conditions. This inherent divergence of derivatives effectively controls not only the thermodynamic, electrostatic, and transport properties of water, but they also influence on transport and chemical processes in SCW systems. The behavior of water as solvent, with some simplification, one can describe by following way while the subcritical water is good solvent for inorganic and bad solvent for organic materials, it turns into the opposite in the SC region; it could dissolve several organic materials but could not dissolve some inorganic ones. By using pure SCW, after days or months various corrosion products can still be dissolved into it.

Both compressibility and thermal expansion behaviour are very important factors in order to understand the shifts of the equilibrium constant in supercritical solvents as a system response on both thermal and mechanical perturbations. The coefficient of isothermal compressibility is defined as:

$$\beta = \frac{1}{\rho}\left(\frac{\delta\rho}{\delta p}\right)_T, \tag{2.2}$$

and diverges sharply (critical exponent ~ 1.241) from ideal gas values to infinity at the critical point. It is an interesting fact that the β divergence depends on pathways of approaching to the critical state along the critical isochore (sharpest slope) or

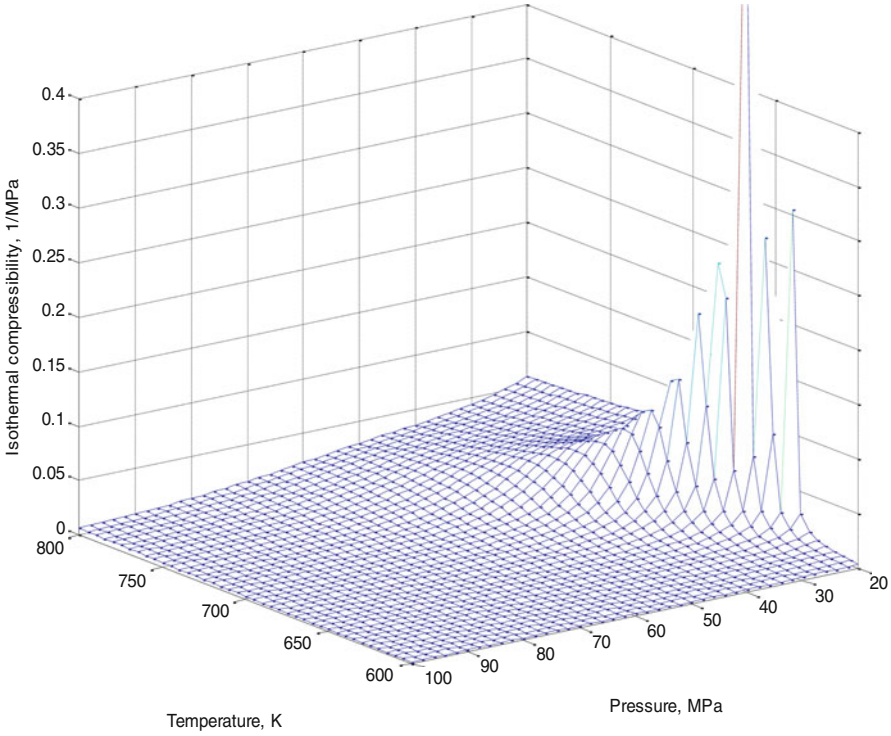

Fig. 2.2 $\beta - p - T$ – surface of supercritical water

along any other pathway in the *p-T* plane. There are three major regions in which it is possible to mark the *p-T* plane (Fig. 2.2):

- the low-density region along an isobar at $T > 723$ K where the isothermal compressibility decreases with both pressure and temperature;
- a region to the low-density side along an isotherm where the isothermal compressibility increases with pressure and decreases with temperature;
- a region to the high-density side along an isobar where the isothermal compressibility decreases with pressure and increases with temperature.

In supercritical fluid, the isothermal compressibility in the low-density region is typically several times larger than those in the high-density region. The coefficient of isobaric expansion is defined as:

$$\alpha_T = -\frac{1}{\rho}\left(\frac{\delta\rho}{\delta T}\right)_p. \tag{2.3}$$

The qualitative behaviour of the α_T *(p,T)* and β*(p,T)* surfaces is similar, but relative maxima of α_T along the isotherms and isobars are shifted to larger densities

relative to β. Isochoric heat capacity behaviour, like isothermal compressibility and isobaric expansion, changes from ideal gas values to infinity at the critical point.

In contrast to the strong divergence of the isothermal compressibility and isobaric expansion, the C_V has a near logarithmic divergence. Supercritical maxima of isochoric heat capacities in the pressure – temperature diagram tend to go to the side of decreasing density. At pressures less than 30 MPa, and temperatures less than 673.15 K, the surface C_V *(p,T)* looks like to the isothermal compressibility β. Isobaric heat capacity from thermodynamic relationships is

$$C_P = C_V + T\frac{\alpha_T^2}{\rho\beta}. \tag{2.4}$$

The near-critical region has the similar asymptotic behaviour for all fluids and theoretically is described by the universal critical exponents and scaling functions, and is based on the scaling concept. The power laws, that represent asymptotic behaviour along the iso-lines on thermodynamic surfaces, are described in numerous literature sources. The main conclusion is that – H_2O behaviour is not unusual in critical region and has the same anomalies as all other fluids.

2.4 Local Extrema of Thermodynamic Properties. The Widom Line

Thermal effects and volume changes of reactions are linearly dependent on compressibility behavior of fluids. Local extrema in α_T, β and ρ have a significant influence on the nature of both heat and mass transport processes. As an example, for the design of high-pressure units for SCW biomass treatment the local rate of convection heat transfer is proportional to both fluid flux and C_P. Usually fluid flux is also proportional to α_T and ρ. Therefore, the maximum flow rates occur at state conditions intermediate between α_T and ρ maxima. Because C_P is a function of α_T, its extreme projections are nearly coincident. As a result, convection heat transfer rates in supercritical conditions attain local maxima in the vicinity of α_T extremes. Near the critical point, the extrema lines for response functions are merged. An asymptotic line as continuation of vapour pressure curve to the one phase region is often named – the Widom line often referred as pseudo-critical or pseudo-spinodal line. The extrema lines (isobaric heat capacity – C_P, compressibility coefficients – α_T and β, speed of sound – *a,* inflection points – *IP*, the Joule – Thomson coefficient – λ) were calculated on the basis of the Wagner and Pruss equation of state [8]. A quantitative presentation of extreme behavior in the properties of H_2O in the $P - T$ diagram is illustrated in Fig. 2.3.

The pressure range, where all extrema lines are merged, is located within 22 ... 25 MPa. Similar picture giving the same lines for water with fittings based on IAPWS EoS is considered in [16]. The main conclusion from these calculations is as follows. No universal curve as continuation of vapor pressure curve exists.

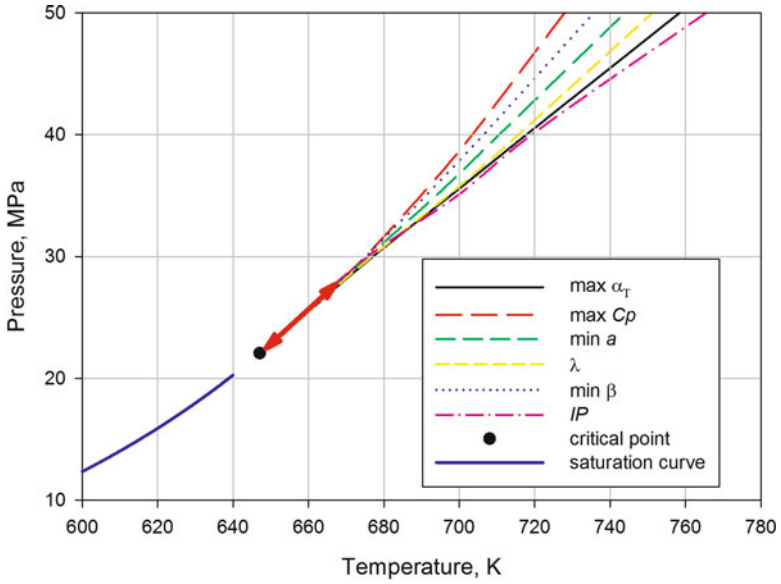

Fig. 2.3 Extrema of response functions in the $P - T$ diagram

In practical design of SCW units, we need to consider non-purity of water. It leads to a shift of extrema lines in the pressure – temperature plane. The typical impurity in supercritical water is a small concentration of NaCl. To study the changes in behaviour along the Widom line, we have calculated the shift of the max C_P line at different concentrations (100, 200, and 300 ppm) [17]. We suggested that at small concentrations of NaCl in water the correspondence state principle is working. The NaCl additives displace the position of critical point along critical line of aqueous solution (Fig. 2.4). Detailed analysis of data was given by Shibue [18]. Critical temperatures and critical pressures of aqueous NaCl solutions also were taken from [18].

To those versed in the art, it is known that enhanced solubility is able to accelerate reaction rates, particularly supercritical water can be a medium for either ionic or single-radical chemistry. A variety of compounds are hardly soluble, if at all, in a medium at room temperature, however they could become soluble in super critical media. Contrary to this observation, those compounds that are soluble in media at room temperature could become less soluble at supercritical conditions.

Solubility growth in water – salt systems at supercritical conditions plays a principal role for the SCW biomass treatment and other industrial applications. Experimental data on solubility of solids in supercritical water have testified that pressure increases the solubility of most of the solids above the H_2O critical temperature (systems H_2O–SiO_2, H_2O–Na_2SO_4, H_2O–Li_2SO_4, etc. are examples confirming this observation). At the present time, there are many computer programs for modelling salt/water systems, taking into account the irreversible dissolution

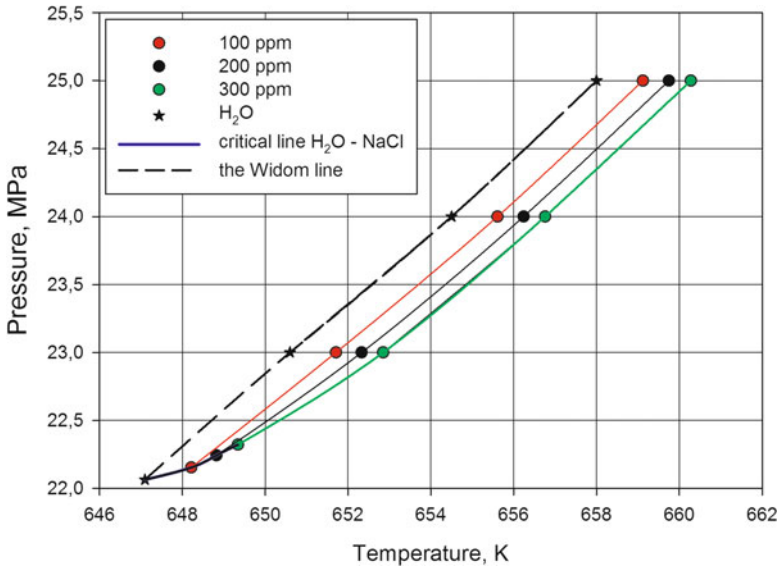

Fig. 2.4 Shift of critical point and max C_P lines in aqueous solution of NaCl [17]

of the reactants and the reversible precipitation of secondary products. From a mathematical point of view, the most successful approach to calculate the equilibrium assemblage is based upon a solution of a set of non-linear mass-action equations, involving equilibrium constants for all relevant equilibrium and auxiliary sets of linear mass-balance and charge balance equations. The primary aim of computer programs is to calculate the speciation of aqueous solutions and their equilibrium to salts (e.g., http://h2o.usgs.gov/software). Most comprehensive review of experimental data on aqueous phase equilibria and solution properties at elevated temperatures and pressures is given by Valyashko [19].

2.5 Phase Equilibria in Binary Mixtures. Global Phase Diagram

Theoretical analysis of the topology of phase diagrams is a very useful tool for understanding the phenomena of phase equilibrium that are observed in biomass components – supercritical water mixtures in vicinity of the Widom line. The pioneering work of van Konynenburg and Scott [20] demonstrated that the van der Waals one-fluid model has opened opportunities of qualitative reproducing the main types of phase diagrams of binary fluids. The proposed classification was successful, and is now used as a basis for describing the different types of phase behavior in binary mixtures. At present, the topological analysis of equilibrium surfaces of binary fluid systems contains 26 singularities and 56 scenarios of

evolution of the p–T diagrams [21]. The introduction of liquid–solid equilibria into classification schemes makes it possible to outline a strategy of continuous topological transformation for constructing complete phase diagrams. The mapping of the global surface of a thermodynamic equilibrium onto the space of parameters of an equation of state gives the possibility to obtain the most comprehensive system of criteria for predicting of the binary mixture phase behaviour. The influence of critical parameters of compounds on phase topology is visualized via global phase diagrams. Such diagrams are presented not in the pressure – temperature variables but in the space of the equation of state parameters, e.g. the van der Waals geometric – b and energetic – a parameters or critical parameters.

For understanding and classifying a great number of phase diagrams, the determination of critical points is an important practical and theoretical problem. A mixture of a given composition can have one, more than one, or none critical point. The types of phase behavior that are of interest for the SCW technologies are characterized as follows (Fig. 2.5).

(I) The simplest type that has a continuous critical curve between the two critical points C_1 and C_2. It can shape of the critical curve and the position of the azeotropic line.

(II) This type is characterized by the presence of an immiscibility zone at temperatures below the critical temperature of a more volatile component, by a critical curve that connects two critical points of pure components, and by a critical line that starts from the critical end point where the liquid–liquid equilibrium line ends.

(III) This type comprises two different critical curves. One of them starts from the critical point of a pure component with a higher critical temperature and goes to the range of high pressures. The other critical curve starts from the critical point of the other component and leads to the critical end point at the end of the three-phase line. The type is divided into five subtypes. The main subtypes differ in the arrangement of the three-phase line at pressures above the saturation pressure of components and the azeotropic line that is bounded by the azeotropic end point from below and by the critical azeotropic point from above (subtype III–A). A distinctive feature for subtype III–H is the occurrence of azeotropy.

(IV) Type IV is characterized by two curves of the liquid–liquid–gas equilibrium. The high temperature three-phase line is bounded by two critical end points (lower (LCEP) and upper (UCEP)). In the vicinity of the UCEP, the solution becomes immiscible with decreasing temperature. In the region of the LCEP, an immiscibility zone appears with increasing temperature.

(V) This type resembles type IV which has no liquid–liquid critical line and three-phase line at low temperatures. For this type, the occurrence of azeotropic states and multiextremal critical lines is possible.

(VI) This type of phase behavior is characterized by the liquid–vapor critical line that connects two critical points of pure components and by the liquid–liquid critical line with a pressure peak that connects the UCEP and the LCEP in the three-phase line.

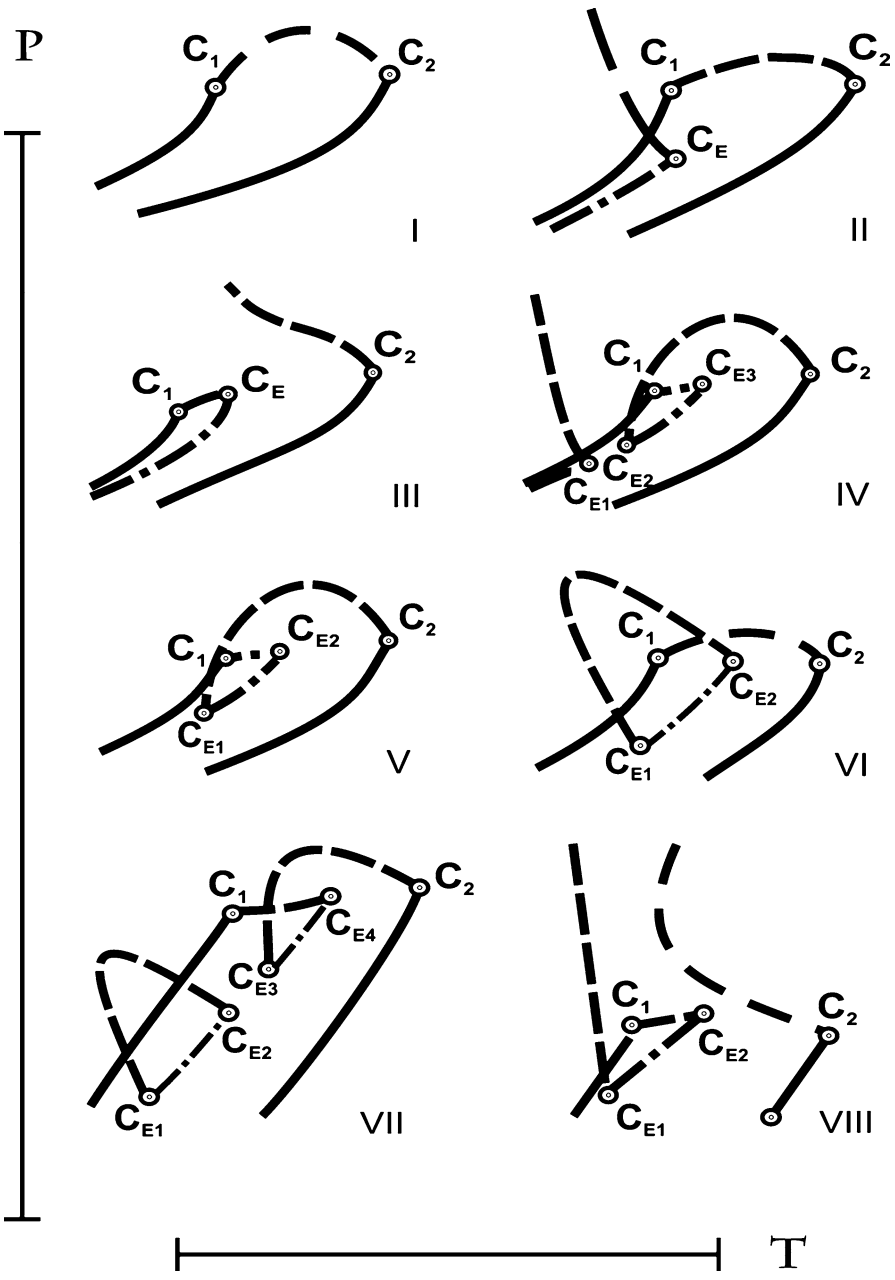

Fig. 2.5 Types of phase diagrams: C_1 are critical points of pure components; C_{E1} mean the critical end points; the *continuous line* denotes the equilibrium curves of pure components; the *dashed lines* correspond the critical lines; and the *dash-dotted lines* denote the three-phase equilibrium curves

(VII) This type, unlike I–VI, has not been confirmed experimentally and differs from type VI by the behavior of the liquid–vapor critical curve, which is divided into two lines that start at the critical points of pure components and end at the LCEP and UCEP in the second three-phase line.

(VIII) This type is characterized by three critical lines. One critical line starts at the critical point of one of the pure components and goes towards the range of high pressures as in type III. The other critical curves start at the LCEP and UCEP in the three-phase line and end in the region of infinitely high pressures and the critical point of the other pure component, respectively.

The systems of interests, for example, H_2O + n-alkanes, $H_2O + CO_2$ belong to the type III phase diagrams according to van Konynenburg and Scott [20], with three phase equilibrium and interrupted critical line, of which the lower branch connects the critical point of n-alkane and the upper critical end point and the upper branch runs from the critical point of pure water to high pressures (valid to water – n – hexacosane). Other systems include H_2, CH_4, CO_2 and etc. Figs. 2.6 and 2.7 illustrate collection of experimentally determined critical curves of aqueous systems.

The system SCW – O_2. The critical curve, an envelope of the isopleths, begins at the critical point of water (647 K), has a temperature minimum (639 K) at about 75 MPa and proceeds to 250 MPa at 659 K. Excess volume, V^E, values have been calculated for 673 K from 30 to 250 MPa. All V^E values are positive. The maximum is 57 $cm^3\ mol^{-1}$ at 70 mol % of H_2O at 30 MPa and about 2 $cm^3\ mol^{-1}$ at 40 mol % H_2O and 250 MPa [22].

The water-carbon dioxide system exhibits type III phase behavior in the classification of van Konynenburg and Scott [20] with a discontinuous vapor–liquid critical curve, a wide region of liquid–liquid coexistence below the critical temperature of CO_2, and very limited mutual solubility in the regions of two- and three-phase equilibria. This system was studied by Takenouchi and Kennedy [23] to pressures of 160 MPa and at temperatures of 383–623 K. The critical curve of the system trends toward higher pressures at lower temperatures and departs strongly from the critical point of pure water. At low pressures the CO_2 rich phase is the light phase, but at higher pressures this phase is the denser fluid phase. In a natural system of H_2O–CO_2 complete miscibility will not exist below 538 K; at higher temperatures a completely mixed supercritical fluid may exist, but at lower temperatures this fluid will segregate into two fluid phases. Fluid-fluid equilibria and critical curves in the system H_2O–CO_2 have been studied, among others by Tödheide and Franck [24], Heidemann and Khalil [25] and Blencoe et al. [26].

The water – nitrogen system has been investigated by Tsiklis and Maslennikova [27], Prokhorova and Tsiklis [28], Japas and Franck [29]. Despite some differences in $p - T - x$ conditions, the phase diagram topology of the three systems is not changed. The available data indicate that immiscibility is generally restricted to temperature below about 673 K. The critical curves consistently exhibit temperature minima. These minima occur at 60–70 MPa and $\sim$ 638 K in the H_2O–N_2 system [29], and in vicinity 155–190 MPa and $\sim$ 538 K in the H_2O–CO_2 system [25].

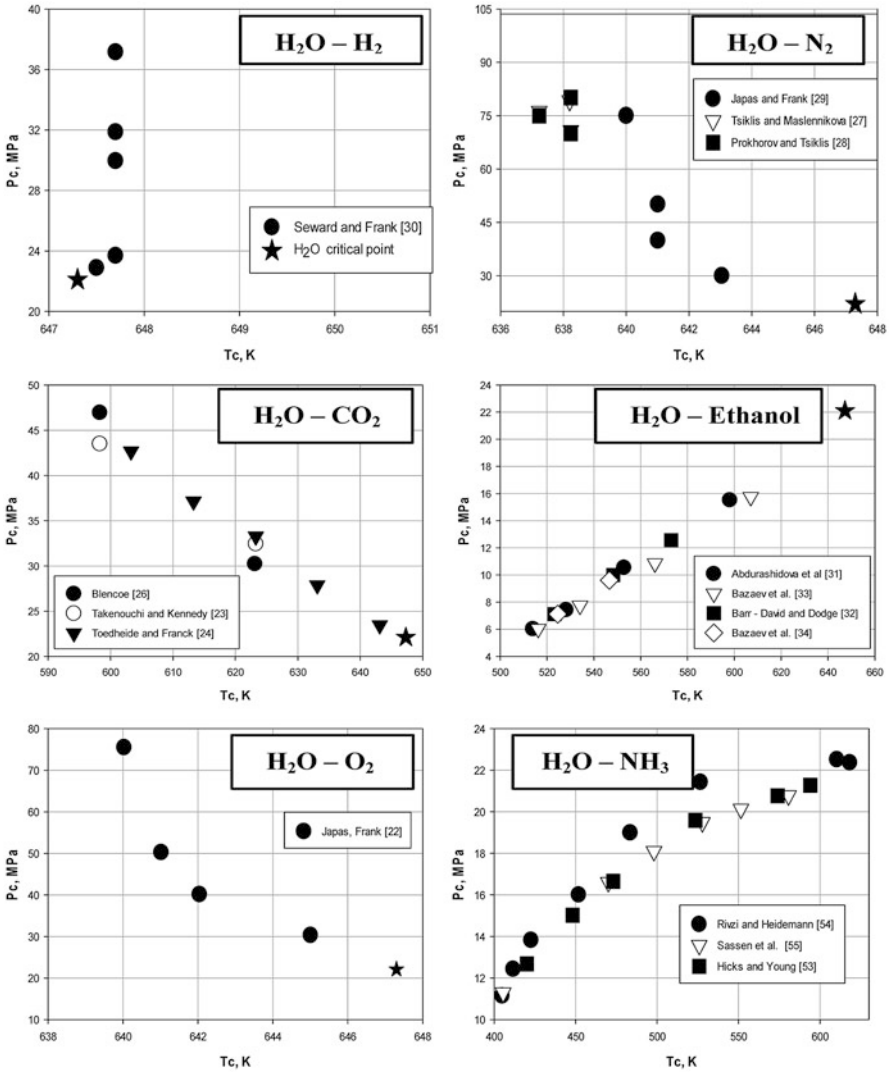

Fig. 2.6 Experimental $P - T$ data along critical curve for the SCW – key biomass component binary mixtures

The system SCW – H_2 has been studied isochorically from 0.5 to 90 mol-% H_2 and up to 713 K and 250 MPa pressure using an autoclave containing two sapphire windows through which phase transitions could be observed at elevated temperatures and pressures. The system was found to exhibit so-called "gas-gas" immiscibility with a critical curve proceeding to higher temperatures and pressures from the critical point of pure water. Within the range of these experiments, the

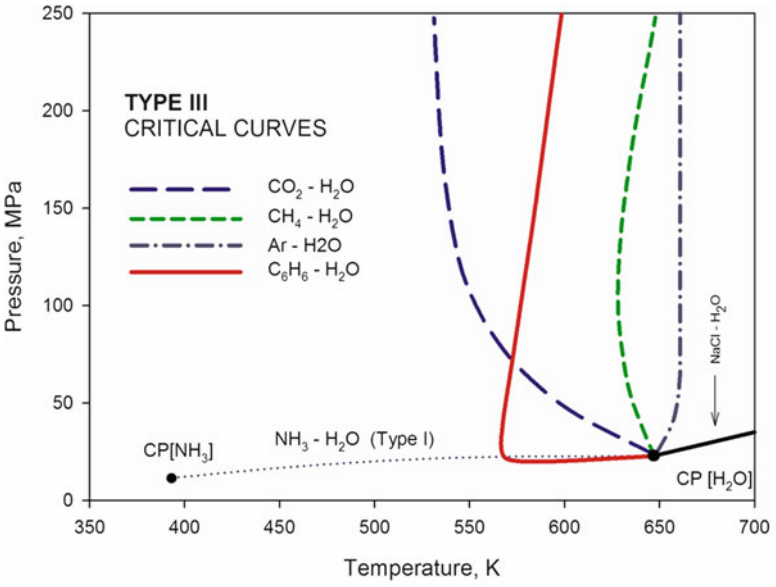

Fig. 2.7 Collection of experimentally determined critical curves of aqueous systems

critical temperature of H_2–H_2O mixtures does not change any noticeable from that of pure water (e.g. $T_c = 654.5$ K at $p_c = 25.2$ MPa for 38 mol % H_2) [30].

The system water – ethanol at temperatures up to 673.15 K, including the saturation curve and the critical and supercritical regions, and at pressures up to 50 MPa for ethanol concentrations of 0.2, 0.5, and 0.8 mole fractions was studied particularly by Abdurashidova et al. [31]. The data of p, ρ, T, x – measurements are used to determine the critical parameters of mixtures. The thermal decomposition of ethanol molecules is observed at a temperature above 623.15 K [31–34]. Both systems water – ammonia [53–55] and water – ethanol [31–34] are a classic example of simplest type I of phase behavior. We should emphasize that, although presented in the context of key components, the topics tackled could apply to thermodynamic models of other biomass components.

Theoretical comprehension of the topology of fluid phase equilibrium has proven to be very useful for the description of complex fluid phase relations, which are observed in multiple-component systems. Indeed, whereas the phase diagram of a one-component system is very simple, at least eight different types of phase diagrams have already been observed for binary systems. Many studies have shown that equations of state are able to generate the different kinds of fluid phase equilibrium (liquid-vapour, liquid-liquid, gas-gas and liquid-liquid-gas). The first pioneering work of this type was the study of van Konynenburg and Scott [20]. They have shown that the simplest van der Waals model reproduces qualitatively the major types of phase diagrams of binary fluids. A classification was proposed and is currently used as a basis, for the discrimination of different kinds of phase diagrams,

in binary systems. Following Varchenko's approach [35], generic phenomena encountered in binary mixtures when the pressure p and the temperature T change, correspond to singularities of the convex envelope (with respect to the x variable) of the "front" (a multifunction of the variable x) representing the Gibbs potential $G(p,T,x)$. Pressure p and temperature T play the role of external model parameters like k_{12}. Although there are no theoretical limits in the extension of this approach for three- or multiple-component mixtures, classification studies – even for ternaries – are just at their beginning because of the amount of work that has to be carried out.

Our aim is to recognise a wide variety of phase diagrams from analysis of variations in geometry and energy characteristics (e.g., in critical volume and critical temperature) of mixture components. The influence of these two parameters on the phase diagram topology could be conveniently visualised on the master diagram, called a "*global phase diagram*". Such a diagram shows the different areas of occurrence of the possible phase diagrams as a function of the geometry and energy factors of the compounds used. Ever since the work of van Konynenburg and Scott [20], numerous studies have been carried out on other, more realistic EoS [36, 37]. The global phase diagrams of such different models, as the one-fluid **EoS** of binary Lennard-Jones fluids [36] and the Redlich-Kwong model [37], are almost identical in their main features including such a sensitive phenomenon as the closed-loops of liquid-liquid immiscibility. Therefore, most of the considerations and conclusions made on the basis of one of the realistic models can be transferred vice versa.

The boundaries, between the various types in the global phase diagram, can be calculated directly using the thermodynamic description of the boundary states (tri-critical line, double critical end-points, etc.). The dimensionless co-ordinates that are used for the representation of the boundary states, depend on the equation of state model, but normally they are designed similar to those proposed by van Konynenburg and Scott for the van der Waals model [20]. In this case, the global phase diagrams of all realistic models have a very similar structure, in particular for the case of equal sized molecules. We consider here the classical Redlich-Kwong model as an example.

The Redlich-Kwong EoS [6] is used in its classical, non-modified, form:

$$p = \frac{RT}{(V-b)} - \frac{a}{T^{0.5}V\,(V-b)}, \tag{2.5}$$

where **R** is the universal gas constant, and parameters a and b of the mixture **EoS** depend on the mole fractions x_i and x_j of the components i and j and on the corresponding parameters a_{ij} and b_{ij} for different pairs of interacting molecules:

$$\begin{aligned} a &= \sum_{i=1}^{2}\sum_{j=1}^{2} x_i x_j a_{ij} \\ b &= \sum_{i=1}^{2}\sum x_i x_j b_{ij}\,. \end{aligned} \tag{2.6}$$

The set of dimensionless parameters for the Redlich-Kwong model is as follows [37]:

$$Z_1 = \frac{d_{22} - d_{11}}{d_{22} + d_{11}},$$
$$Z_2 = \frac{d_{22} - 2d_{12} + d_{11}}{d_{22} + d_{11}},$$
$$Z_3 = \frac{b_{22} - b_{11}}{b_{22} + b_{11}},$$
$$Z_4 = \frac{b_{22} - 2b_{12} + b_{11}}{b_{22} + b_{11}} \tag{2.7}$$

where

$$d_{ij} = \frac{T_{ij}^* b_{ij}}{b_{ii} b_{jj}},\quad T_{ij}^* = \left(\frac{\Omega_b a_{ij}}{R\Omega_a b_{ij}}\right)^{2/3},\quad \Omega_a = \left[9\left(2^{1/3} - 1\right)\right]^{-1},\quad \Omega_b = \frac{2^{1/3} - 1}{3}. \tag{2.8}$$

It should be brought to the attention that the dimensionless parameter Z_1 represents the difference of the critical pressures of the components, and that the dimensionless parameter Z_3 represents the difference of the critical volumes. So, there is a direct correlation of the global phase behaviour between mixtures and critical properties, i.e. geometry and energy parameters of real binary fluids.

Recently, Cismondi and Michelsen [38] introduced a procedure to generate different type of phase diagrams classified by van Konynenburg and Scott. Their strategy does not take into account an existence of solid phase. At present time Patel and Sunol [39] developed an automated and reliable procedure for systematic generation of global phase diagrams for binary systems. The approach utilizes equation of state, incorporates solid phase and is successful in generation of type VI phase diagram. The procedure enables automatic generation of GPD which incorporates calculations of all important landmarks such as critical endpoints (*CEP*), quadruple point (*QP*, if any), critical azeotropic points (*CAP*), azeotropic endpoints (*AEP*), pure azeotropic points (*PAP*), critical line, liquid–liquid–vapor line (*L*1*L*2*V*, if any), solid–liquid–liquid line (*SL*1*L*2, if any), solid–liquid–vapor line (*SLV*) and azeotropic line. The proposed strategy is completely general in that it does not require any knowledge about the type of phase diagram and can be applied to any pressure explicit equation of state model. Figure 2.8 shows the global phase diagram for binary mixtures of equal-sized molecules, plotted in the two-dimensional $(Z_1 - Z_2)$ space [40].

The simplest boundary is a normal critical point when two fluid phases are becoming identical. Critical conditions are expressed in terms of the molar Gibbs energy derivatives in the following way:

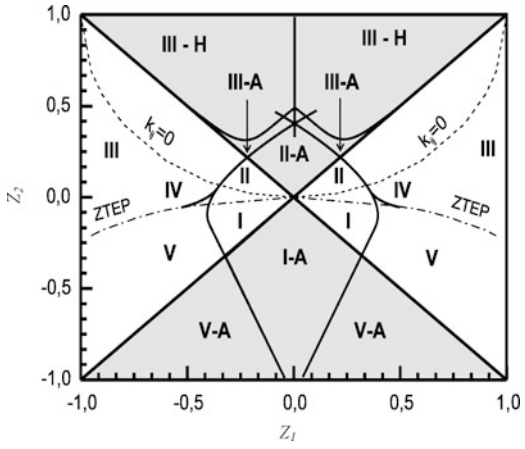

Fig. 2.8 Global phase diagram of the Redlich-Kwong model

$$\left(\frac{\partial^2 G}{\partial x^2}\right)_{p,T} = \left(\frac{\partial^3 G}{\partial x^3}\right)_{p,T} = 0. \tag{2.9}$$

Corresponding critical conditions for the composition – temperature – volume variables are:

$$\begin{aligned} &A_{xx} - WA_{xV} = 0; \\ &A_{xxx} - 3WA_{xxV} + 3W^2 A_{xVV} - 3W^3 A_{VVV} = 0; \end{aligned} \tag{2.10}$$

where A is the molar Helmholtz energy,

$W = \frac{A_{xx}}{A_{VV}}$, $A_{mVnx} = \left(\frac{\partial^{n+m} A}{\partial x^n \partial V^m}\right)_T$ is a contracted notation for differentiation operation which can be solved for V_C and T_C at given concentration x.

Without exception, one of the most important boundaries is visualised by the tri-critical points (TCP). This boundary divides the classes I and V, II and IV, or III and IV. The tri-critical state is a state, where the regions of the liquid-liquid-gas immiscibility shrink to one point, which is named the TCP. Three phases become identical at a TCP. Another important boundary in the global phase diagrams is the locus of double critical end-points (DCEP) that divides types III and IV, or II and IV. Type IV is characterised by two liquid-liquid-gas curves. One is at high temperatures and is restricted by two critical end points [one lower critical end point (LCEP) and an upper critical end point (UCEP)]. At the upper critical end point, the solution (compounds) become(s) immiscible as the temperature is lowered. At a lower critical end point, the solution separates into two phases as the temperature is increased. A DCEP occurs in a type IV when LCEP high-temperature three-phase region joins the UCEP of low-temperature three-phase region. A DCEP is produced in a type III system when the critical curve cuts tangentially the three-phase line in a pressure – temperature diagram. The types I and II, or IV and V, differ in the existence of a three-phase line, which goes from high pressures to an

UCEP. For this case, the boundary situation is defined by the zero-temperature end point (ZTEP). Thermodynamic expressions and mathematical tools are given in the literature [37, 38].

Azeotropy in binary fluids can be easily predicted in the framework of global phase diagrams. The corresponding boundary situation is called the degenerated critical azeotropic point (CAP) and represents the limit of the critical azeotropy at $x_i \to 0$ or at $x_i \to 1$. This results in solving the system of thermodynamic equations for a degenerated critical azeotrope.

One may obtain the relationships for azeotropy boundaries from the global phase diagram [shaded **A** (Azeotropy) and **H** (Hetero-azeotropy)] regions in Fig. 2.8. The above azeotropic borders are straight lines in the (Z_1, Z_2)-plane that cross at a single point in the vicinity of the centre for equal sized molecules. It opens the opportunity for obtaining the series of inequalities to separate azeotropic and non-azeotropic regions of the global phase diagram. For the Redlich – Kwong EoS a corresponding relationship was obtained in an analytical form [41]:

$$Z_2 = \mp Z_1 - (1 \pm Z_1)\left(\frac{1 - Z_4}{1 \pm Z_3} - 1\right) 0.6731. \tag{2.11}$$

Global phase diagrams of binary fluids represent the boundaries between different types of phase behaviour in a dimensionless parameter space. In a real $P - T - x$ space, two relatively similar components usually have an uninterrupted critical curve between the two critical points of the pure components. An upper branch extends from the critical point of the higher boiling component to higher pressures, sometimes passing through a temperature minimum as in the C_6H_6–H_2O system.

A general simplification of the theoretical description of ternary mixtures has been achieved by the consideration of the water + salt system as a single component mixture. This component has interaction parameters (or EoS parameters) dependent on the concentration of the salt. The details of the water-salt interactions have to be taken as averaged by an effective, spherically symmetric, interaction potential. This approach is justified by the phase behaviour of the system water + sodium chloride that belongs to the simplest type II of phase behaviour and has a very simple critical curve in the vicinity of the critical point of water. Three main types of phase topologies have been known in binary water-electrolyte systems. These are type-III (H_2O–HCl) system where hydrogen chloride is more volatile than water and a negative azeotropic line for water-rich compositions, at pressures below the saturation pressure of the water and the liquid-liquid-gas equilibrium, occur at pressures near saturation pressures of HCl, type-II (H_2O–NaCl, H_2O–NaOH), and type-IV phase diagrams (H_2O–Na_2WO_4, H_2O–K_2SO_4, H_2O–UO_2SO_4).

The topological predictions on the basis of a global phase diagram will become a convenient method in the analysis of supercritical water mixtures of scientific and industrial interest. Topologically, there is no difference in isoproperty behaviour for any pure fluid. This fact allows us to find the parameters of the equation of state model, which can reproduce thermodynamic properties of an arbitrary substance in a local region of a phase diagram.

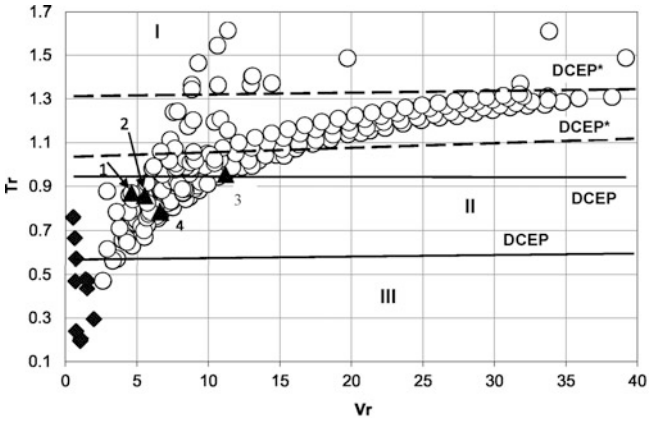

Fig. 2.9 Allocation of phase behavior types for hydrocarbon – water and key biomass components – water mixtures in reduced variables. ▲ – selected aqueous solutions of hydrocarbons performing III type of phase behavior: (*1*) cyclohexane; (*2*) benzene; (*3*) *n*-decane; and (*4*) *n*-hexane [43]; ♦ – selected aqueous solutions of key biomass components

To simulate the behavior of different biomass components in the SCW media, models based on equations of state are more than sufficient. Considering a huge array of reaction products, which wait in queue to be destroyed or recycled, it is obvious that there is need to develop theoretically sound methods for reliable assessment of their thermodynamic and phase behaviour, especially, at supercritical water conditions.

If combination rules are known, then it is possible to determine the global phase diagram via the ratio of critical parameters of pure components only [42]. The boundaries between different types of phase behavior taken from their paper and distribution of reduced critical temperatures and volumes for aqueous solutions of hydrocarbons are given in Fig. 2.9.

Critical parameters of hydrocarbons were taken from correlation [15]. The simple estimation of transition from III type of phase behaviour to II type ($T_r = T_{CH2O}/T_C \approx 0.5$) in terms of pure components for the one fluid model of the Redlich-Kwong EoS [44] and Carnahan-Starling – van der Waals EoS [42] with the Lorentz – Berthelot combination rules ($k_{12} = 0$) shows the serious discrepancies with experimental evidence of III type phase behaviour for systems water – alkanes [45, 46, 43]. Experimental values of k_{12} for water–alkanes systems show significant deviations from zero. Therefore, for a correct classification of phase behavior types, we should shift the lines DCEP to DCEP* (Fig. 2.9), which is achieved due to variations in the interaction parameters k_{12} and l_{12}. The DCEP* lines in Fig. 2.9 classify experimentally observed types of phase behavior more correctly for the SRK model with parameters corresponding the values $k_{12} = 0.1$ and $l_{12} = 0.01$. The Lorentz – Berthelot model is not working also for ammonia water and ethanol – water systems.

The traditional classification of fluid phase behavior can easily be discussed with the aid of the *p-T* projections of fluid phase diagrams. There are two kinds of phase diagrams. Phase diagrams of types I, V, and VI have the vapour pressure curves that are started and ended in nonvariant points with equilibria where the no solid phase exist. In the case of types II, III and IV, some critical curves, starting in high-temperature nonvariant points, are not ended by the nonvariant points from the lower temperature side, where the solid phase should exist. A solid phase is absent in calculations of fluid phase diagrams using previously discussed equations of state and the nonvariant equilibria with solid could not be obtained even at 0 K. Therefore the monovariant curves remain incomplete on the theoretical $p - T$ projections. As a result these diagrams can be considered as the *'derivative' versions.* It demonstrates not only the main types of fluid phase behavior but also the fluid phase diagrams which appear when the heterogeneous fluid equilibria are bounded not only by another fluid equilibrium but also by the equilibrium with solid phase that is usually observed in the most real systems [47].

To give an exhaustive description of phase behavior in binary systems, the systematic classification of the main types of *complete phase diagrams* that considers any equilibria between liquid, gas and/or solid phases in a wide range of temperatures and pressures was proposed by V. Valyashko [47].

In the new nomenclature, suggested by Valyashko [48] for systematic classification of binary complete phase diagrams, four main types of fluid phase behavior are designated in order of their continuous topological transformation as ***a, b, c*** and ***d*** types. In order to simplify the construction of phase diagrams he accepted the following limitations for the main types of binary complete phase diagrams:

1. The melting temperature of the pure nonvolatile component is higher than the critical temperature of the volatile component.
2. There are no solid-phase transformations such as polymorphism, formation of solid solutions and compounds, and azeotropy in liquid-gas equilibria in the systems under consideration.
3. Liquid immiscibility is terminated by the critical region at high pressures and cannot be represented by more than two separated immiscibility regions of different types.

Complete phase diagram presentation is very sophisticated and we refer the readers to the cited original Valyashko's papers.

The design and development of SCW technology depend on the ability to model and predict accurately the solid-supercritical fluid equilibrium. It has been known for more than 100 years that a supercritical fluid can dissolve a substance of low volatility and that the solubility is dependent on the pressure. The ability to control solubility by means of pressure as well as temperature has brought about the use of supercritical fluids in different applications. For SCW technologies, knowledge of the solubility of substances in supercritical fluids is very important and a large number of experimental data has become available in recent years.

Hence, a more correct estimation of binary interaction parameters is needed to predict phase behaviour of biomass components in supercritical water. The best

Table 2.3 Recommended values of the Krichevskii parameters for biomass component solutes

Solute	A_{Kr}, MPa [50]	A_{Kr}, MPa [49]
H_2	169.9 ± 7.8	170 ± 8
N_2	177.5 ± 7.1	178 ± 7
O_2	171.3 ± 7.3	177 ± 10
CO	173.3 ± 5	174 ± 10
CO_2	124.3 ± 5	127 ± 10
NH_3	42 ± 1	46 ± 5
CH_4	164.6 ± 5.7	164 ± 6
Methanol	32 ± 6	29 ± 5
Ethanol	43 ± 2	44 ± 5

source of information for model parameter determination to restore critical curves in the SCW – biomass component mixtures is experimental data in vicinity of solution critical line. In dilute near-critical solutions, the partial molar properties of solutes, the coordinates of the critical lines of binary mixtures, and the temperature variations of the vapor–liquid distribution and Henry's constants, are controlled by the critical value of the derivative $A_{Kr} = -\left(\frac{\partial A}{\partial V \partial x}\right)^c_{T,x=0} = \left(\frac{\partial P}{\partial x}\right)^c_{T,V,x=0}$ which is called the Krichevskii parameter.

Here A is the Helmholtz energy of the binary system, x is the mole fraction of a solute, P is the pressure, V is the volume of the system, and the superscript c indicates evaluation at the solvent critical point. The Krichevskii parameter is finite and has the dimension of pressure. The physical meaning of the Krichevskii parameter is that it gives the change in pressure at the critical point of the solvent when an infinitesimal amount of solvent molecules is replaced by solute at constant volume and temperature: for most neutral solutes the pressure will rise, and for solutes with strong attractions to the solvent (for example, ions in water) the pressure of the system will decrease [49]. The review of Fernández-Prini et al. [50] presents data for 14 gases (He, Ne, Ar, Kr, Xe, H_2, N_2, O_2, CO, CO_2, H_2S, CH_4, C_2H_6, SF_6) in water with the accuracy of 2–6 % at high temperatures; similar uncertainties are expected for derived *AKr* results. Most comprehensive review of the significance of the Krichevskii parameter for the analysis of the phase equilibria, including the solubility, in binary systems are presented by Plyasunov [49]. Recommended values of the Krichevskii parameters for selected biomass components from [49] and [50] are given in Table 2.3.

2.6 Uncertainties and Conflicts in the Parameter Estimation for Thermodynamic Models

The reliable estimation of model parameters from experimental data in phase equilibria simulation is an important requirement in many applications. Such models offer the useful tools of aggregating large amounts of data, allow both data for interpolation of data and extensions beyond regions in which measurements have

been made, and provide insight into physical and chemical phenomena. Transition from real phenomenon to its model entails the appearance of uncertainty caused by the statistical pattern of experimental information, inadequacy and ambiguity of used models, etc. Experimental data, which are generated by different experimental units, have as a rule different dimensions, different physical meaning, and different statistical distribution. It results to conflict situation when the set of parameters restored according to the one category of data does not correspond to parameters from other data sources. Therefore, the conflict appears in model parameter estimation and it is desirable to reduce an arising uncertainty by the simultaneous consideration of all data fitness criteria for each property.

Advanced methods of probability theory consider uncertainty as some specific value, characterizing an emergence of predetermined chance outcomes. Statistical methods interpret all variety of uncertainty types in the framework of the randomness concept. Nevertheless, there are ill-structured situations, which have not any strictly defined boundaries and cannot be accurately formulated. Examples of such situation are standard statements in the problem of model parameter estimation: "mean-square deviation of calculated values from measured data must be in neighborhood of feasible deviations δ" or "to provide the best fit to measured data". The expressions "in neighborhood" or "best fit" have not exact boundaries which separate one class of objects from others. The vague verbal models such as "equation of state is valid in critical point neighborhood", "high temperature approximation", "adequate model", and etc. are fuzzy formulated targets, which depend on biased assessment of boundaries for used approximations.

The problem of optimum parameter estimation in models of thermodynamic and phase behavior under the uncertainty is a multicriteria problem of mathematical programming. The first step in solution of multicriteria problem is a search of the Pareto set, i.e. such compromise domain in the permissible parameter space $\boldsymbol{X}$ where the value of any criterion cannot be improved without the value of the others criteria being worsened. The diverse computational methods of the Pareto-optimum parameter estimation and different (crisp and fuzzy) convolution schemes to reduce a vector criterion into the scalar one should be used. As examples of case study, we demonstrate the Pareto-optimum estimation of parameters in the Soave–Redlich–Kwong equation of state (EoS), using different conflicting data sets (simultaneous description of the phase equilibria and critical line data in binary mixtures).

The last two decades have been characterized by a growing comprehension of the fact that the ideas of uncertainty should not be neglected in the fluid phase equilibria modeling. Since one of the meanings of uncertainty is randomness, a conventional approach is utilized via probability and random process theories. However, as recognized recently, the probabilistic methods are accompanied by serious problems during its implementation in practice of phase equilibria modeling and lead to the unreliable estimation of parameters.

Development of reliable models for thermodynamic and phase behavior description of binary mixtures in most cases is associated with the estimation of the binary interaction parameters from the restricted set of *VLE* data. Although there are rigorous relationships to obtain from EoS model the different derivatives of

thermodynamic values, for instance, the prediction of critical lines from the EoS with parameters restored from *VLE* data is questionable due to diverse sources of uncertainty both in the used models and experimental data.

To illustrate conflict between phase equilibria and critical line description we consider the water – carbon dioxide system in the vicinity of critical point of water. Experimental data on $p - V - T - x$ properties have been taken from [51, 44] data on phase equilibria and critical curve have been extracted from [52, 24]. The critical lines have been calculated using algorithm developed in [25]. We performed phase equilibria and critical line calculations for the SRK EoS with parameters binary interaction parameters k_{12} and l_{12} from standard mixing rules,

$$\begin{aligned} b &= b_{11}x^2 + l_{12}x\,(1-x)\left(\tfrac{b_{11}+b_{22}}{2}\right) + b_{22}\,(1-x)^2 \\ a &= a_{11}x^2 + k_{12}x\,(1-x)\,\sqrt{a_{11}a_{22}} + a_{22}\,(1-x)^2 \end{aligned} \tag{2.12}$$

restored from different crisp convolution schemes.

For simplicity the results of calculation for phase equilibria and critical line are presented in Figs. 2.10 and 2.11 only for additive compromise scheme. The parameters restored from *P-V-T-x* data [51, 44] are not suitable for phase equilibria description and completely unusable for critical curve description. These parameters are skipped here. There are many speculations about problem of EoS singular behavior near critical point. Here we do not discuss the possible approaches to consistent description of regular and singular behavior of thermodynamic functions, but point out only the fact that classical EoS models, which are widely used in phase equilibrium calculations, cannot describe simultaneously phase equilibria and critical curves. The problem of conflict between parameters restored from different sections of thermodynamic surface is remained valid for more sophisticated EoS with singular behavior also. As a whole, it is observed the general conflict situation: if the cross-interaction parameters are restored from the one category of properties the prognosis of other properties is dubious in spite of indubitable validity of thermodynamic relationships. The final solution has subjective nature and depends on the statement of problem and decision maker experience.

2.7 Conclusion

This study is one of the first attempts to establish and demonstrate multiple links existing among the phase equilibria phenomena in supercritical aqueous mixtures with biomass components and their models. From the very beginning of these efforts, the global phase diagrams have been a very useful tool for scientists and engineers working in the field of emerging SCW technologies. There is no doubt that extension of our knowledge about global phase behaviour of two- and multicomponent fluids will lead to the creation of reliable engineering recipes for solving the actual problems of SCW technology applications in biomass conversion.

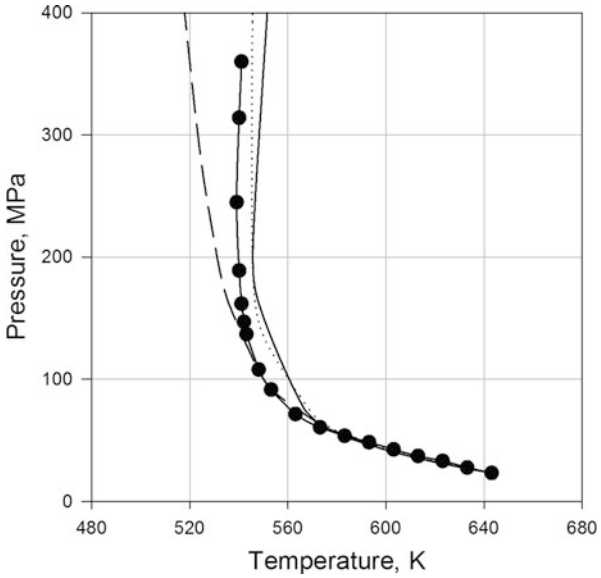

Fig. 2.10 Critical lines of H_2O–CO_2 system. –●– – experimental data [24]. ▬ – best fit of *VLE* data. ○○○○ – compromise solution. ▬ ▬ – best fit of critical curve

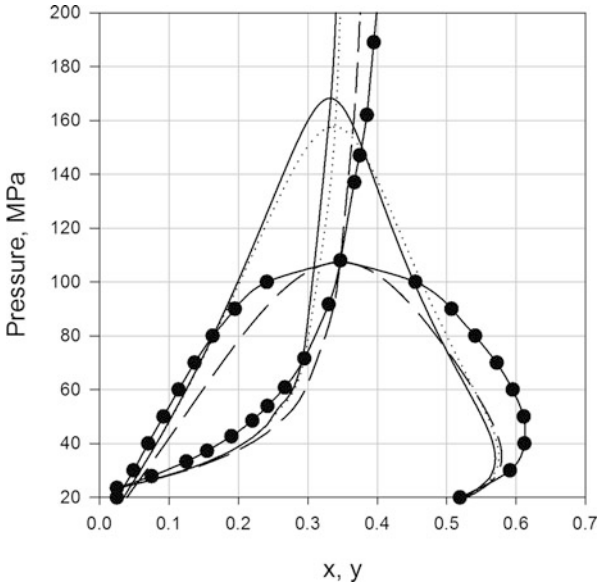

Fig. 2.11 Phase equilibria in H_2O–CO_2 system. –●– – experiment $T = 548.15$ K. ▬ – best fit of *VLE* data. ○○○○ – compromise solution. ▬ ▬ – best fit of critical curve

Unfortunately, there are no rigorous mathematical methods and sound physical concepts to construct the adequate model without enlisting of subjective point of view due to inaccuracy of our knowledge. To minimize this source of unavoidable uncertainty the different compromise schemes of criteria convolution are considered and their selection is strongly depended on decision maker experience. Here, by way of illustration, it has been applied to estimate the Redlich-Kwong-Soave EoS parameters for simultaneous description of the phase equilibria and critical line data in binary mixtures.

References

1. Peterson A, Vogel F, Lachance R, Froling M, Antal M, Tester J. Thermochemical biofuel production in hydrothermal media: a review of sub- and supercritical water technologies. Energy Environ Sci. 2008;1:32–65.
2. Smith Jr RL, Fang Z. Properties and phase equilibria of fluid mixtures as the basis for developing green chemical processes. Fluid Phase Equilibria. 2011;302:65–73.
3. Dorrestijn E, Laarhoven L, Arends I, Mulder P. The occurrence and reactivity of phenoxyl linkages in lignin and low rank coal. J Anal Appl Pyrolysis. 2000;54:153–92.
4. ECN. Phyllis, database for biomass and waste. 2012; Available from: http://www.ecn.nl/phyllis2
5. Peng D-Y, Robinson DB. A new two-constant equation of state. Ind Eng Chem Fundam. 1976;15:59–64.
6. Redlich O, Kwong JNS. On the thermodynamics of solutions V. An equation of state. Fugacities of gaseous solutions. Chem Rev. 1949;44:233–44.
7. Soave G. Equilibrium constants from a modified Redlich–Kwong equation of state. Chem Eng Sci. 1972;27:1197–2003.
8. Wagner W, Pruß A. The IAPWS formulation 1995 for the thermodynamic properties of ordinary water substance for general and scientific use. J Phys Chem Ref Data. 2002;31(2):387–535.
9. Joback K. Knowledge bases for computerized physical property estimation. Fluid Phase Equilibria. 2001;185:45–52.
10. Somayajulu GR. Estimation procedures for critical constants. J Chem Eng Data. 1989;34(1):106–20.
11. Labanowski JK, Motoc I, Damkoehler RA. The physical meaning of tological indexes. Comput Chem. 1991;15:47–53.
12. Katritzky AR, Dobchev D, Karelson M. Physical, chemical, and technological property correlation with chemical structure: the potential of QSPR. Z Naturforsch. 2006;61b:373–84.
13. Rogers D, Hopfinger AJ. Applications of genetic function approximation (GFA) to quantitative structure-activity relationships (QSAR) and quantitative structure property relationships (QSPR). J Chem Inf Comp Sci. 1994;34:854–66.
14. Mosier P, Jurs P. QSAR/QSPR studies using probabilistic neural networks and generalized regression neural networks. J Chem Inf Comput Sci. 2002;42(6):1460–70.
15. Wakeham W, Cholakov G, Roumiana S. Liquid density and critical properties of hydrocarbons estimated from molecular structure. J Chem Eng Data. 2002;47:559–70.
16. Imre A, Deiters U, Kraska T, Tiselj I. The pseudocritical regions for supercritical water. Nucl Eng Des. 2012;252:179–83.
17. Imre A, Hazi A, Horvath MC, Mazur V, Artemenko S. The effect of low-concentration inorganic materials on the behaviour of supercritical water. Nucl Eng Des. 2011;241:296–300.

18. Shibue Y. Vapor pressures of aqueous NaCl and $CaCl_2$ solutions at elevated temperatures. Fluid Phase Equilibria. 2003;213(1–2):39–51.
19. Valyashko V. Experimental data on aqueous phase equilibria and solution properties at elevated temperatures and pressures. New York: Wiley; 2009.
20. van Konynenburg PH, Scott RL. Critical lines and phase equilibria in binary van der Waals mixtures. Philos Trans R Soc Lond. 1980;298:495–540.
21. Aicardi F, Valentin P, Ferrand E. On the classification of generic phenomena in one–parameter families of thermodynamic binary mixtures. Phys Chem Chem Phys. 2002;4:884–95.
22. Japas M, Franck E. High pressure phase equilibria and *PVT*-data of the water-oxygen system including water-Air to 673 K and 250 MPa. Ber Bunsenges Phys Chem. 1985;89:1268–75.
23. Takenouchi S, Kennedy GC. The binary system H_2O–CO_2 at high temperatures and pressures. Am J Sci. 1964;262:1055–74.
24. Todheide K, Frank E. Das zweiphasengebiet und die kritische kurve im system kohlendioxid-wasser bis zu drucken von 3500 bar. Z Phys Chem. 1963;37:387–401.
25. Heidemann R, Khalil A. The calculation of critical points. AICHE J. 1980;26:769–78.
26. Blencoe JG. The CO_2–H_2O system: IV. Empirical, isothermal equations for representing vapor–liquid equilibria at 110–350 °C, P < =150 MPa. Am Mineral. 2004;89(10):1447–55.
27. Tsiklis DS, Maslennikova VY. Limited mutual solubility of the gases in the H_2O–N_2 system. Dokl Akad Nauk SSSR. 1965;161:645–7.
28. Prokhorova VM, Tsiklis DS. Gas-gas equilibrium in nitrogen-water system. Russ J Phys Chem. 1970;44:1173.
29. Japas ML, Franck EU. High pressure phase equilibria and PVT data of the water – nitrogen system to 673 K and 250 MPa. Ber Bunsenges Phys Chem. 1985;89:793–800.
30. Seward TM, Franck EU. The system hydrogen – water up to 440 °C and 2500 bar pressure. Ber Bunsenges Phys Chem. 1981;85:2–8.
31. Abdurashidova A, Bazaev A, Bazaev E, Abdulagatov I. The thermal properties of water-ethanol system in the near-critical and supercritical states. High Temp. 2007;45(2):178–86.
32. Barr-David F, Dodge BF. Vapor-liquid equilibrium at high pressures. The systems ethanol-water and 2-propanol-water. J Chem Eng Data. 1959;4:107–21.
33. Bazaev AR, Abdulagatov IM, Magee JW, Bazaev EA, Ramazanova AE, Abdurashidova AA. PVTx measurements for a H_2O + methanol mixture in the subcritical and supercritical regions. Int J Thermophys. 2004;25:805–38.
34. Bazaev EA, Bazaev AR, Abdurashidova AA. An experimental investigation of the critical state of aqueous solutions of aliphatic alcohols. High Temp. 2009;47:195–200.
35. Varchenko AN. Evolution of convex hulls and phase transition in thermodynamics. J Sov Math. 1990;52(4):3305–25.
36. Mazur VA, Boshkov LZ, Murakhovsky VG. Global phase behaviour of binary mixtures of Lennard–Jones molecules. Phys Lett. 1984;104A:415–8.
37. Deiters UK, Pegg JL. Systematic investigation of the phase behavior of binary fluid mixtures. I. Calculations based on the Redlich–Kwong equation of state. J Chem Phys. 1989;90:6632–41.
38. Cismondi M, Michelsen M. Global phase equilibrium calculations: critical lines, critical end points and liquid-liquid-vapour equilibrium in binary mixtures. J Supercrit Fluids. 2007;39(3):287–95.
39. Patel K, Sunol A. Automatic generation of global phase equilibrium diagrams for binary systems from equations of state. Comput Chem Eng. 2009;33:1793–800.
40. Mazur V, Boshkov L, Artemenko S. Global phase behaviour of *natural* refrigerant mixtures. In: Proceedings of the IIR – Gustav Lorentzen conference: natural working fluids. Oslo; 1998. p. 495–504.
41. Artemenko S, Mazur V. Azeotropy in the natural and synthetic refrigerant mixtures. Int J Refrig. 2007;30:831–9.
42. Sadus R, Wang J. Phase behaviour of binary mixtures: a global phase diagram solely in terms of pure component properties. Fluid Phase Equilibria. 2003;214:67–78.

43. Brunner E, Thies M, Schneider G. Fluid mixtures at high pressures: phase behavior and critical phenomena for binary mixtures of water with aromatic hydrocarbons. J Supercrit Fluids. 2006;39:160–73.
44. Shmulovich KI, Mazur VA, Kalinichev AG, Khodorevskaya LI. P-V-T and component activity-concentration relations for systems of H_2O-nonpolar gas type. Geochem Int. 1980;17(6):18–31.
45. Tsonopoulos C, Wilson GM. Phase behavior of binary mixtures: a global phase diagram solely in terms of pure component properties. AICHE J. 1983;29(6):990–3.
46. Tsonopulos C. Thermodynamic analysis of the mutual solubilities of normal alkanes and water. Fluid Phase Equilibria. 1999;156:21–33.
47. Valyashko VM. Derivation of complete phase diagrams for ternary systems with immiscibility phenomena and solid–fluid equilibria. Pure Appl Chem. 2002;74(10):1871–84.
48. Valyashko V. Hydrothermal properties of materials. Experimental data on aqueous phase equilibria and solution properties at elevated temperatures and pressures. New York: Wiley; 2008. p. 1–134.
49. Plyasunov A. Values of the Krichevskii parameter, AKr, of aqueous nonelectrolytes evaluated from relevant experimental data. J Phys Chem Ref Data. 2012;41(3):1–27.
50. Fernández-Prini R, Alvarez JL, Harvey AH. Henry's constant and vapor – liquid distribution constants for gaseous solutes in H_2O and D_2O at high temperatures. J Phys Chem Ref Data. 2003;32:903–16.
51. Sterner M, Bodnar R. Synthetic fluid inclusions. X: experimental determination of P – V – T – x properties in the CO_2–H_2O system to 6 KB and 700 C. Am J Sci. 1991;64:1–54.
52. Mather A, Franck E. Phase equilibria in the system carbon dioxide-water at elevated pressures. J Phys Chem. 1992;6:6–8.
53. Hicks CP, Young CL. The gas-liquid critical properties of binary mixtures. Chem Rev. 1975;75(2):119–75.
54. Rizvi SSH, Heidemann RA. Vapor- liquid equilibrium in the ammonia – water system. J Chem Eng Data. 1987;32:183–91.
55. Sassen CL, van Kwartel RAC, van der Kooi HJ, de Swaan AJ. Vapor – liquid equilibrium for the system ammonia + water up to the critical region. J Chem Eng Data. 1990;35:140–4.

http://www.springer.com/978-94-017-8922-6

Near-critical and Supercritical Water and Their Applications for Biorefineries

Fan, K.; Xu, C.C. (Eds.)

2014, XVI, 474 p. 134 illus., 53 illus. in color., Hardcover
ISBN: 978-94-017-8922-6